Folia Neuropathologica

Could lipid CH_2/CH_3 analysis by *in vivo* ^{1}H MRS help in differentiation of tumor recurrence and post-radiation effects?

Łukasz Matulewicz[1], Maria Sokół[1], Jerzy Wydmański[2], Leszek Hawrylewicz[3]

[1]Department of Medical Physics, Maria Skłodowska-Curie Memorial Cancer Center and Institute of Oncology, Gliwice Branch, Poland;
[2]Department of Radiotherapy, Maria Skłodowska-Curie Memorial Cancer Center and Institute of Oncology, Gliwice Branch, Poland;
[3]Department of Radiotherapy and Brachytherapy Planning, Maria Skłodowska-Curie Memorial Cancer Center and Institute of Oncology, Gliwice Branch, Poland

Folia Neuropathol 2006; 44 (2): 116-124

Abstract

Purpose: *To inspect the potential diagnostic role of in vivo ^{1}H MRS lipid methylene CH_2 to methyl CH_3 signal ratio in differentiation of recurrent brain tumor from radiation injury.*
Methods: *Two patients – one with documented recurrence and the other without recurrence – were monitored by means of ^{1}H MRS before and during two years after radiation therapy. The comparative group consisted of 20 patients with glial tumor recurrence diagnosed 2 years after the radiotherapy.*
Results: *In case of tumor recurrence, an increase of the lipid CH_2/CH_3 value is observed. In contrast, for the patient with no tumor recurrence and within the brain areas distant from the tumor the CH_2/CH_3 ratio reveals a negative correlation vs. time after irradiation. The Lip trend to increase on radiotherapy both at the tumor bed and within the non-involved areas lessens the value of Lip as a marker of tumor recurrence.*
Conclusion: *The analysis of the lipid CH_2/CH_3 ratio may be useful in differentiation of the tumor recurrence from radiation response.*
The Lip signals observed in normally appearing brain tissue after radiotherapy could originate from the change of metabolism of irradiated cells.

Key words: *proton magnetic resonance spectroscopy, brain tumor, radiotherapy, lipids*

Introduction

Radiation therapy plays a central role in the treatment of malignant gliomas, and is considered to be the most effective adjuvant therapy following surgery. Although the recent advances of the irradiation techniques have made the irradiation more safe for the tissues that are distant from the tumor, the radiation exposure of the healthy brain cannot be completely eliminated. That provides a unique opportunity to study the effect of radiation on normal brain tissue by means of ^{1}H MRS *in vivo*.

On the other hand, in the target area treatment related brain necrosis is a dose-limiting factor for

Communicating author:
Łukasz Matulewicz, Department of Medical Physics, Maria Skłodowska-Curie Memorial Cancer Center and Institute of Oncology, ul. Wybrzeże AK 15, 44-100 Gliwice, Poland, tel. +48 32 278 80 47, fax +48 32 231 35 12, e-mail: lukasz.matulewicz@io.gliwice.pl

either conventional or stereotactic radiotherapy. Morphologic changes seen in computed tomographic and magnetic resonance images are, however, insufficient to discriminate radiation-induced changes from tumor recurrence [31]. Complementary methods, such as ^{1}H MR spectroscopy (MRS) or ^{1}H MRS imaging (MRSI), seem to give an opportunity for a better insight into an altered brain metabolism following treatment. However, as revealed from the ^{1}H MRS studies, when basing upon the cholines to N-acetylaspartate ratio (Cho/NAA) and that of the cholines to the total creatine (Cho/Cr), the sensitivity of tumor differentiation from necrosis is less than 80% [26]. The use of MRS imaging improves the accuracy, but also in the case of ^{1}H MRSI it was noticed that in the subacute stage of radiation necrosis Cho levels may be elevated and thus leading to misdiagnosis [9]. Thus, monitoring of the main signal intensities, like NAA, choline, creatine, etc. seems to be insufficient for differentiation of cerebral necrosis from recurrent/residual tumor, which means that an additional parameter is required to improve the sensitivity.

Methods

Two patients were treated with radiotherapy in the Center of Oncology Maria Skłodowska-Curie Memorial Institute Branch in Gliwice (patient 1 received treatment comprising brachytherapy and fractionated external-beam radiotherapy whereas patient 2 received fractionated external-beam radiotherapy) and were followed using MRI and ^{1}H MRS scans before and during 24 months after irradiation.

Table I. Characteristics of patients

Patient No.	Age	Sex	Histologic diagnosis	Lesion location
1	26	M	Astrocytoma	left frontal lobe
2	50	M	Astrocytoma	left occipital lobe
3	28	M	Astrocytoma	right temporal lobe
4	50	M	Astrocytoma	left frontal lobe
5	55	M	Astrocytoma	left frontal lobe
6	43	M	Astrocytoma	left occipital lobe
7	46	F	Astrocytoma	left occipital lobe
8	48	M	Astrocytoma anaplasticum	right occipital lobe
9	37	M	Astrocytoma anaplasticum	left temporal lobe
10	52	F	Astrocytoma anaplasticum	right frontal lobe
11	38	M	Astrocytoma anaplasticum	left occipital lobe
12	38	M	Astrocytoma anaplasticum	left occipital lobe
13	38	F	Oligoastrocytoma anaplasticum	left frontal lobe
14	64	F	Oligoastrocytoma anaplasticum	left frontal lobe
15	55	M	Gliobastoma multiforme	left temporal lobe
16	53	M	Gliobastoma multiforme	right parietal lobe
17	47	M	Gliobastoma multiforme	left temporal lobe
18	50	F	Gliobastoma multiforme	left temporal lobe
19	57	M	Gliobastoma multiforme	right occipital lobe
20	32	M	Gliobastoma multiforme	left temporal lobe

The comparative group (COM group) comprises 20 patients (mean age 45±19). The inclusion criterion was the local recurrence of the tumor up to two years after radiotherapy. The patients' characteristics are collected in Table I.

The whole-body 2T MRI/MRS system (Elscint 2T Prestige) equipped with a standard head coil and operating at a proton resonance frequency of 81.3 MHz was used.

^{1}H MR spectra were acquired using a single voxel double-spin echo PRESS sequence with the parameters: TR 1500 ms, TE 35 ms, 50 acquisitions, and a 1.5 x 1.5 x 1.5 cm^3 for the voxel volume. The acquisition was preceded by the global and local shimming procedure. Water suppression was achieved using the chemical shift selective saturation (CHESS) technique.

The MRS examinations were performed successively during several months after the radiotherapy completion. The end of radiotherapy is denoted here as the "0" day of the MRS observation.

Localized spectra were acquired from two volumes of interest (VOIs) – always the same during the whole study. The first VOI was located at the tumor bed and the second one within an unaffected tissue in the contralateral side of the brain, as showed in Figures 1-2.

Similarly, in the case of the COM group the spectra were obtained from the tumor lobe and contralaterally.

The spectra were normalized to 1 in the range of 0-4.2 ppm and then post-processed with the automatic fitting in the frequency domain using the residuals method offered by PeakFit 4.0 (SPSS Inc., Chicago, USA). The set of fitted signals was the same for all the spectra under study. The details of the procedure are given in reference [27].

The mobile lipids were analyzed using two independent methods. In the first approach the ratio of the methylene group lipid signal at 1.30 ppm to that due to the methyl groups at 0.92 ppm (CH_2/CH_3), the most representative lipid signals, was analyzed.

In the second approach the contribution of the mobile lipids signals (Lip) into the NMR spectrum was estimated by a calculation of an integral intensity of the whole lipid band in the range 0.7-1.39 ppm (the lactate doublet at 1.26 and 1.35 ppm as well as that due to alanine (1.44 and 1.50 ppm) were excluded from the calculation).

Resonances originating from macromolecules, such as cytosolic proteins, and other membrane-bound and/or partially immobilized compounds were not involved in calculations.

The statistical comparisons were done using the Mann-Whitney U test and the Wicoxon Matched Pairs test.

Case reports and results

Patient 1

A 26-year-old man who suffered from a progressive weakness of the right limbs, dysphasia and recent memory disturbance for 6 months. Magnetic resonance (MR) brain scan revealed a 3.5 cm expansive lesion in the left frontal lobe. The tumor was non-operable. The patient underwent stereotactic tumor biopsy and the implantation of the catheters was performed. The histological diagnosis was anaplastic astrocytoma grade 3. Over three days a radiation dose of 15 Gy was delivered at a depth of 5 mm from catheters surface. After brachytherapy the patient received a total dose of 50 Gy in 25 fractions to the tumor volume with a margin of 3 cm. MRI scanning revealed tumor progression 9 months after the treatment completion. The patient was operated palliatively 10 months after RT. His follow-up is 2 years (on months 2, 6, 14, 18 and 24 after irradiation).

Patient 2

A 18-year-old woman, the first disease symptoms were epileptic seizure and loss of consciousness. MR imaging showed a 3 cm tumor in the right parietal lobe. The operation was radical. The final diagnosis was confirmed by a histopathological examination as oligodendroglioma grade 2. The preoperative tumor volume with a margin of 2 cm was irradiated to a total dose of 54 Gy in 30 fractions. No recurrence features were found in the MRI examinations. The patient follow-up is 2 years (on months 6, 12, 18 and 24 after irradiation). She is in a good general state.

Although the patients being compared suffer from different histological types of the tumors, present results of genetic studies indicate that similarity may exist between oligodendrogliomas and astrocytomas [12]. Moreover, the NMR characteristics as well as tumor cellularity are the same in both histologic glioma types [30].

Figures 1 and 2 show the MR images, treatment plans as well the stack spectra acquired from the tumor lobe during the 2-year follow-up of both the patients included in this report.

Since the standard analysis of the spectra involving the calculation of main metabolite ratios, such as N-acetylaspartate to total creatine (tCr), cholines to tCr, myoInositol to tCr, glutamine and glutamate to tCr and lipids to tCr ratios provided equivocal results and revealed to be useless for the differential diagnosis, we decided to include additional parameters, such as lipid methylene (at 1.3 ppm) CH_2 to lipid methyl (0.9 ppm) CH_3 ratio.

In case of patient 1, the decrease of the CH_2/CH_3 ratio vs. time is preserved only for the voxel located contralaterally to the tumor bed (Fig. 1A and 3A). In the vicinity of the tumor bed the CH_2/CH_3 ratio vs. time is found to increase continuously attaining after 6 months the value being about 3 times higher than at the "0" day (Fig. 3A and Fig. 1B). It is worth noting that for patient 1 the recurrence was diagnosed 9 months after treatment on the basis of MRI and the histopathological analysis. Thus, the spectroscopic observation of the CH_2/CH_3 ratio increase at the tumor bed precedes the MRI indications of the tumor recurrence in over two months. Interestingly, after the

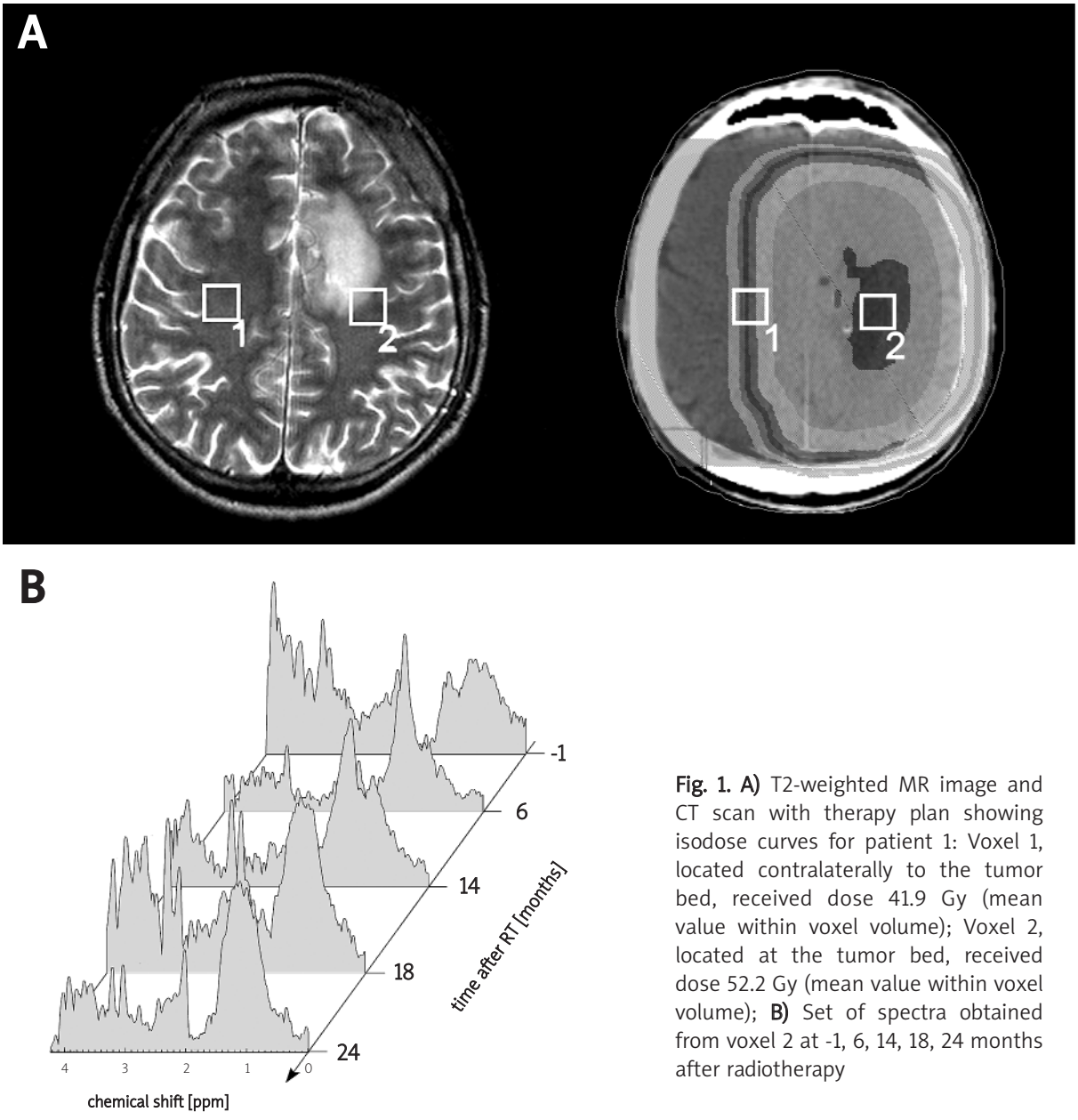

Fig. 1. A) T2-weighted MR image and CT scan with therapy plan showing isodose curves for patient 1: Voxel 1, located contralaterally to the tumor bed, received dose 41.9 Gy (mean value within voxel volume); Voxel 2, located at the tumor bed, received dose 52.2 Gy (mean value within voxel volume); **B)** Set of spectra obtained from voxel 2 at -1, 6, 14, 18, 24 months after radiotherapy

operation the CH_2/CH_3 lipid ratio is found to reduce down to the value close to that for the unaffected contralateral brain. For the tumor bed voxel the variations in the CH_2/CH_3 ratio vs. time are accompanied by the variations in the integral intensity of the band due to mobile visible lipids (Fig. 3B; patient 1). The behavior of the CH_2/CH_3 ratio and Lip, as observed at the tumor bed, seems to correlate with the patient 1 disease history. For both the patients under study the Lip integrated intensities measured in the contralateral VOIs increase vs. time almost linearly (Fig. 3B).

For the patient with no recurrence (patient 2), a linear negative correlation of the lipid CH_2/CH_3 ratio vs. time after irradiation is seen for both the brain areas under study (Fig. 2 and 3A).

The CH_2/CH_3 ratios collected for the COM group consisting of 20 recurrent patients reveal similar trends (Fig. 4A). The individual CH_2/CH_3 tumor lobe values are higher than those obtained for the contralateral regions, and the mean CH_2/CH_3 lobe value, 2.67±1.10 (mean±SD), is significantly higher than the contralateral one, 0.99±0.51 ($p<0.005$). In

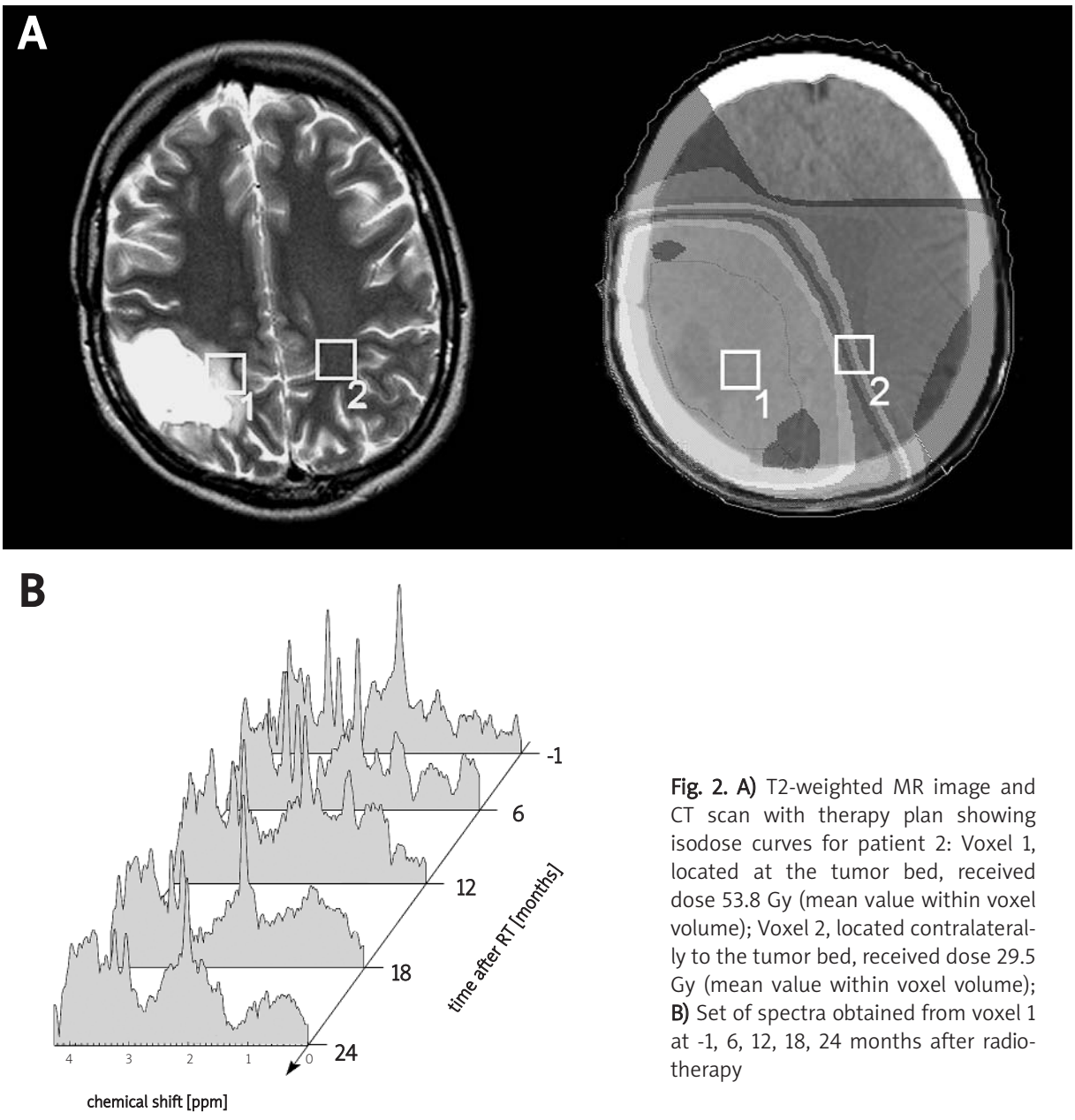

Fig. 2. A) T2-weighted MR image and CT scan with therapy plan showing isodose curves for patient 2: Voxel 1, located at the tumor bed, received dose 53.8 Gy (mean value within voxel volume); Voxel 2, located contralaterally to the tumor bed, received dose 29.5 Gy (mean value within voxel volume); **B)** Set of spectra obtained from voxel 1 at -1, 6, 12, 18, 24 months after radiotherapy

contrast, there are no such clear relations between Lip values calculated for the both analyzed brain regions (Fig. 4B). The mean Lip lobe value, 19.15±8.77, is close to the contralateral one, 15.03±9.13 ($p>0.1$).

Discussion

Metabolic changes induced by radiation are not very different from those induced by tumor recurrence or progression. Thus, a problem of differentiation of

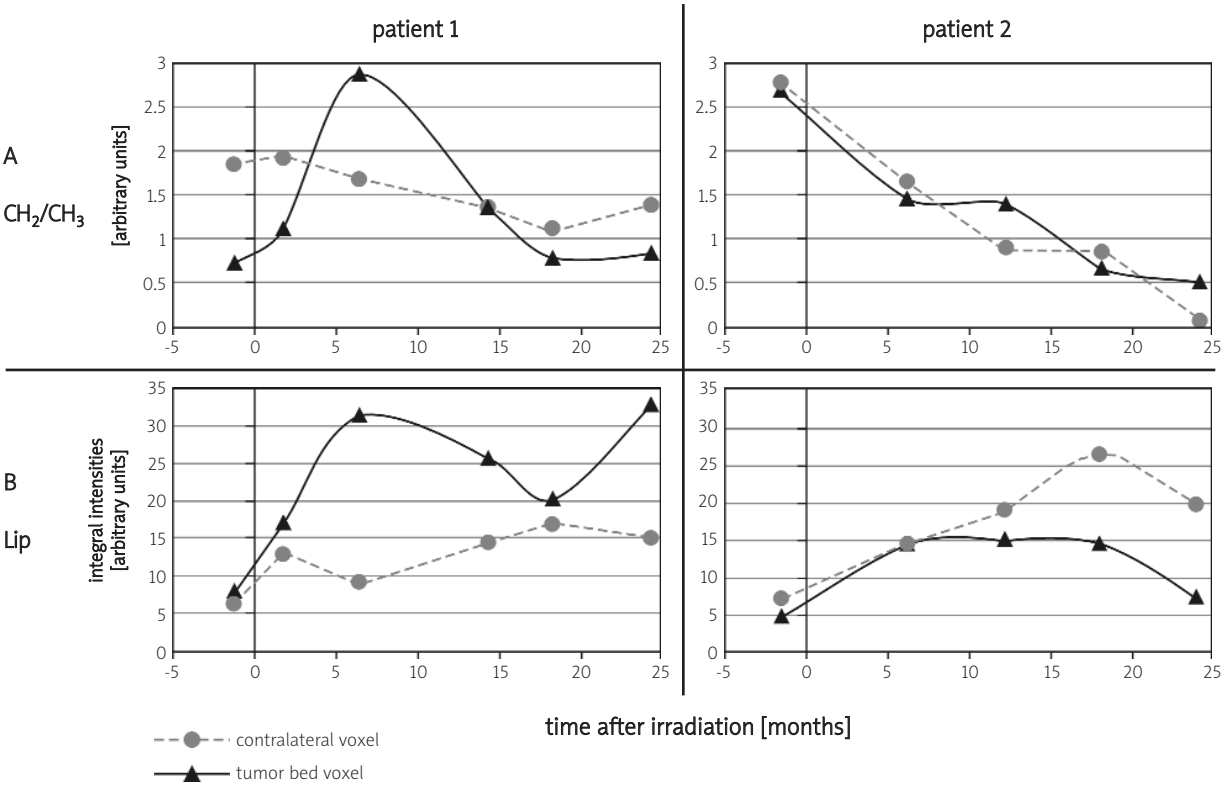

Fig. 3. Lipids CH_2/CH_3 **(A)**, and Lip **(B)** vs. time after irradiation for patients 1 and 2. Time "0" denotes the end of irradiation cycle

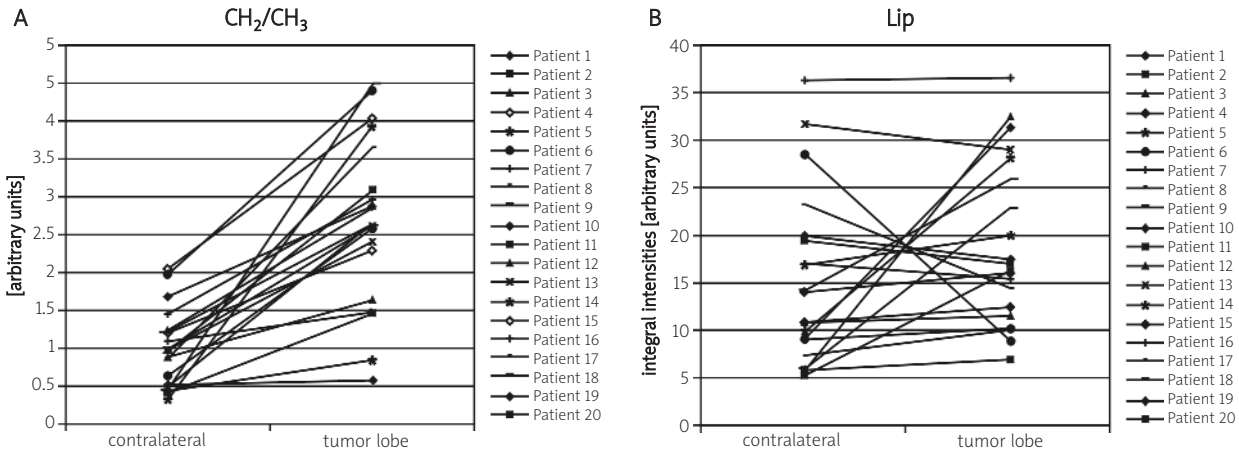

Fig. 4. Lipids CH_2/CH_3 **(A)** and Lip values **(B)** for 20 patients obtained from contralateral and tumor voxels

radiation damage from tumor induced changes by means of MRS is not trivial in case of patients irradiated after brain surgery. While monitoring main NMR signals, like NAA, choline and creatine, some radiation effects may be misinterpreted as tumor – as for instance increased Cho levels in the subacute stage of radiation necrosis [9,16], whereas those due to tumor may be taken as a radiation necrosis [4,26].

If the metabolite ratios are equivocal, MR spectroscopy may still help in the differential diagnosis based on the analysis of the lipid band. In normal spectra, the lipid signals are usually difficult to detect because of signal broadening resulting from restricted mobility of Lip molecules involved in cell membrane formation. Severe damage of cell membranes – due to irradiation and/or tumor development – may release more mobile lipid macromolecules so the Lip signals may be resolved [14]. The mobile lipids have been associated directly to transformed cells and often have been considered as markers of the tumor state itself [15,19].

Recently, it was confirmed that the lipids signals not only increase progressively with tumor grade but that there is also a correlation between the fraction of microscopic necrosis and their integral intensity, as observed *ex vivo* using ^{1}H MRS [21]. The large concentrations of lipid in tumors mean that rapid MRS investigations could contribute to the grading, prognosis and assessment of treatment response [20].

In order to inspect changes occurring within several months of study in the aliphatic region of NMR spectra corresponding to the visible lipid, two complementary approaches of the lipid signals analysis have been compared: using the CH_2/CH_3 ratio (Fig. 3A) and the Lip integral intensity (Fig. 3B). Numerous studies have described the presence of the resonances at about 0.9 and 1.3 ppm in the proton NMR spectra obtained from tumor tissue. These resonances, not detected in the proton spectra of normal brain, arise from terminal methyl, $-CH_3$, and methylene, $(-CH_2-)_n$, groups of fatty acyl chains of the two neutral lipids triglyceride and cholesteryl ester, and have commonly been associated with ongoing cell death processes [1,6,18,24,28]. The integral intensity of the $(-CH_2-)_n$ signal is claimed to depend on the increment of the plasma membrane lipids mobility and/or lipid droplets forming as a result of cell destruction processes.

Hakumaki et al. [10] reported an increase in the methylene peak at 1.3 ppm and also in that due to the methyl groups at 0.9 ppm in treated tumors in animal model *in vivo* (rat brain glioma). In case of high grade human gliomas both signals are found to be higher than in lower grade gliomas, but the CH_2/CH_3 ratio is reduced with respect to those in lipomas or subcutaneous fat, which indicates a much shorter hydrocarbon chain length [8].

In vitro ^{1}H MRS studies indicate that dynamic and/or compositional change of the plasma membrane appears to account for the increase in the CH_2/CH_3 ratio and its value correlates with the fraction of apoptotic cells [2]. Although it is difficult to compare directly the *in vitro* spectral data with that obtained *in vivo*, however the similarity of the time courses of spectral changes observed by Blankenberg et. al within lipids chemical shifts range and those seen by us for the recurrent patient 1 (Fig. 1B) seem to be intriguing [2].

As revealed from our data, early delayed injury, which manifests itself by transient demyelination and occurs from 1 to 6 months after irradiation [32], seems to strongly influence the CH_2/CH_3 ratio – its almost linear decrease in the non-neoplastic peritumoral brain (Fig. 3A; patient 2) and in the contralateral regions (Fig. 3A; patient 1 and 2) is presumably due to the post-radiation effects. In case of a recurrent tumor (Fig. 3A; patient 1) the length of lipid chain sequences represented by the CH_2/CH_3 ratio is found to increase markedly, which may reflect a glioma transformation [7,13,17,20].

The data collected for the COM group including 20 recurrent patients seems to validate the results obtained for patients 1 and 2 – in case of all the recurrences the CH_2/CH_3 ratios calculated from the spectra acquired at the tumor lobe are significantly higher that those obtained contralaterally, where mainly the radiation induced changes take place (the mean values ±SD are 2.67±1.10 and 0.99±0.51, respectively; $p<0.005$) (Fig. 4A). That lipid CH_2/CH_3 value obtained by us for the tumor voxels is close to that obtained by Opstad et al. for glioblastomas (2.6±0.6) [23].

Although, the majority of authors confine the analysis of the spectra to the main metabolites, such as NAA, Cho Cr and mI [3,4,7,29] there are an increasing number of studies addressing the lipid component [5,11,17,21,22]. Our earlier study performed on a large group of irradiated patients showed the lipid levels to increase markedly on irradiation both at the tumor bed and in the noninvolved brain lobe [25]. The present data collected during the long-lasting follow-

up of the irradiated patients confirm these observations. The Lip level increases during several months after radiotherapy completion, both at the tumor bed as well as in the contralateral regions, where the recurrent tumor is highly improbable (Fig. 3B; patients 1 and 2; Fig. 4B). The Lip values at the recurrent area and for the other VOIs are similar – in case of the COM group (Fig. 4B) the mean values at the tumor lobe and contralaterally are 19.15±8.77 and 15.03±9.13, respectively ($p>0.1$), which lessens the value of Lip as a marker of tumor recurrence. Moreover, it follows from the Lip behavior in non-tumor regions that the change of metabolism of irradiated cells could be a probable explanation of the origin of the Lip band observed in normally appearing brain tissue after radiotherapy.

Conclusion

The current study indicates that the analysis of the lipid CH_2/CH_3 ratio may be potentially useful in differentiation of the tumor recurrence from radiation response and incorporation of this parameter into the standard MRS protocol is recommended.

The Lip trend to increase on radiotherapy both at the tumor bed and within the non-involved areas lessens the value of Lip as a marker of tumor recurrence. The Lip signals observed in normally appearing brain tissue after radiotherapy could originate from the change of metabolism of irradiated cells.

References

1. Al-Saffar NM, Titley JC, Robertson D, Clarke PA, Jackson LE, Leach MO, Ronen SM. Apoptosis is associated with triacylglycerol accumulation in Jurkat T-cells. Br J Cancer 2002; 86: 963-970.
2. Blankenberg FG, Katsikis PD, Storrs RW, Beaulieu C, Spielman D, Chen JY, Naumovski L, Tait JF. Quantitative analysis of apoptotic cell death using proton nuclear magnetic resonance spectroscopy. Blood 1997; 89: 3778-3786.
3. Chan YL, Roebuck DJ, Yuen MP, Yeung KW, Lau KY, Li CK, Chik KW. Long-term cerebral metabolite changes on proton magnetic resonance spectroscopy in patients cured of acute lymphoblastic leukemia with previous intrathecal methotrexate and cranial irradiation prophylaxis. Int J Radiat Oncol Biol Phys 2001; 50: 759-763.
4. Chong VF, Rumpel H, Aw YS, Ho GL, Fan YF, Chua EJ. Temporal lobe necrosis following radiation therapy for nasopharyngeal carcinoma: 1H MR spectroscopic findings. Int J Radiat Oncol Biol Phys 1999; 45: 699-705.
5. Chong VF, Rumpel H, Fan YF, Mukherji SK. Temporal lobe changes following radiation therapy: imaging and proton MR spectroscopic findings. Eur Radiol 2001; 11: 317-324.
6. Delikatny EJ, Cooper WA, Brammah S, Sathasivam N, Rideout DC. Nuclear magnetic resonance-visible lipids induced by cationic lipophilic chemotherapeutic agents are accompanied by increased lipid droplet formation and damaged mitochondria. Cancer Res 2002; 62: 1394-1400.
7. Esteve F, Rubin C, Grand S, Kolodie H, Le Bas JF. Transient metabolic changes observed with proton MR spectroscopy in normal human brain after radiation therapy. Int J Radiat Oncol Biol Phys 1998; 40: 279-286.
8. Frund R, Geissler A, Gliese M, Seitz J, Feuerbach S. Magnetic resonance imaging (MRI) and magnetic resonance spectroscopy (MRS) of intracranial lipomas. Front Biosci 1997; 2: f13-f16.
9. Fulham MJ, Bizzi A, Dietz MJ, Shih HH, Raman R, Sobering GS, Frank JA, Dwyer AJ, Alger JR, Di Chiro G. Mapping of brain tumor metabolites with proton MR spectroscopic imaging: clinical relevance. Radiology 1992; 185: 675-686.
10. Hakumaki JM, Poptani H, Sandmair AM, Yla-Herttuala S, Kauppinen RA. 1H MRS detects polyunsaturated fatty acid accumulation during gene therapy of glioma: implications for the in vivo detection of apoptosis. Nat Med 1999; 5: 1323-1327.
11. Heesters MA, Kamman RL, Mooyaart EL, Go KG. Localized proton spectroscopy of inoperable brain gliomas. Response to radiation therapy. J Neurooncol 1993; 17: 27-35.
12. Holland EC, Li Y, Celestino J, Dai C, Schaefer L, Sawaya RA, Fuller GN. Astrocytes give rise to oligodendrogliomas and astrocytomas after gene transfer of polyoma virus middle T antigen in vivo. Am J Pathol 2000; 157: 1031-1037.
13. Kriat M, Vion-Dury J, Confort-Gouny S, Favre R, Viout P, Sciaky M, Sari H, Cozzone PJ. Analysis of plasma lipids by NMR spectroscopy: application to modifications induced by malignant tumors. J Lipid Res 1993; 34: 1009-1019.
14. Kuesel AC, Briere KM, Halliday WC, Sutherland GR, Donnelly SM, Smith IC. Mobile lipid accumulation in necrotic tissue of high grade astrocytomas. Anticancer Res 1996; 16: 1485-1489.
15. Le Moyec L, Tatoud R, Eugene M, Gauville C, Primot I, Charlemagne D, Calvo F. Cell and membrane lipid analysis by proton magnetic resonance spectroscopy in five breast cancer cell lines. Br J Cancer 1992; 66: 623-628.
16. Lee MC, Pirzkall A, McKnight TR, Nelson SJ. 1H-MRSI of radiation effects in normal-appearing white matter: dose-dependence and impact on automated spectral classification. J Magn Reson Imaging 2004; 19: 379-388.
17. Lehnhardt FG, Rohn G, Ernestus RI, Grune M, Hoehn M. 1H- and (31)P-MR spectroscopy of primary and recurrent human brain tumors in vitro: malignancy-characteristic profiles of water soluble and lipophilic spectral components. NMR Biomed 2001; 14: 307-317.
18. Millis KK, Maas WE, Cory DG, Singer S. Gradient, high-resolution, magic-angle spinning nuclear magnetic resonance spectroscopy of human adipocyte tissue. Magn Reson Med 1997; 38: 399-403.
19. Mountford CE, Mackinnon WB. Proton magnetic resonance spectroscopy of lymphocytes: an historical perspective. Immunomethods 1994; 4: 98-112.
20. Murphy PS, Rowland IJ, Viviers L, Brada M, Leach MO, Dzik-Jurasz AS. Could assessment of glioma methylene lipid resonance by in vivo (1)H-MRS be of clinical value? Br J Radiol 2003; 76: 459-463.

21. Negendank W, Li CW, Padavic-Shaller K, Murphy-Boesch J, Brown TR. Phospholipid metabolites in 1H-decoupled 31P MRS in vivo in human cancer: implications for experimental models and clinical studies. Anticancer Res 1996; 16: 1539-1544.
22. Negendank WG, Sauter R, Brown TR, Evelhoch JL, Falini A, Gotsis ED, Heerschap A, Kamada K, Lee BC, Mengeot MM, Moser E, Padavic-Shaller KA, Sanders JA, Spraggins TA, Stillman AE, Terwey B, Vogl TJ, Wicklow K, Zimmerman RA. Proton magnetic resonance spectroscopy in patients with glial tumors: a multicenter study. J Neurosurg 1996; 84: 449-458.
23. Opstad KS, Murphy MM, Wilkins PR, Bell BA, Griffiths JR, Howe FA. Differentiation of metastases from high-grade gliomas using short echo time 1H spectroscopy. J Magn Reson Imaging 2004; 20: 187-192.
24. Rosi A, Luciani AM, Matarrese P, Arancia G, Viti V, Guidoni L. 1H-MRS lipid signal modulation and morphological and ultrastructural changes related to tumor cell proliferation. Magn Reson Med 1999; 42: 248-257.
25. Rutkowski T, Tarnawski R, Sokół M, Maciejewski B. 1H-MR spectroscopy of normal brain tissue before and after postoperative radiotherapy because of primary brain tumors. Int J Radiat Oncol Biol Phys 2003; 56: 1381-1389.
26. Schlemmer HP, Bachert P, Herfarth KK, Zuna I, Debus J, van Kaick G. Proton MR spectroscopic evaluation of suspicious brain lesions after stereotactic radiotherapy. AJNR Am J Neuroradiol 2001; 22: 1316-1324.
27. Sokol M. Analysis of in vivo 1H MR spectra of normal brain tissue by means of second derivative method. Med Sci Monit 2001; 7: 496-503.
28. Tugnoli V, Tosi MR, Tinti A, Trinchero A, Bottura G, Fini G. Characterization of lipids from human brain tissues by multinuclear magnetic resonance spectroscopy. Biopolymers 2001; 62: 297-306.
29. Usenius T, Usenius JP, Tenhunen M, Vainio P, Johansson R, Soimakallio S, Kauppinen R. Radiation-induced changes in human brain metabolites as studied by 1H nuclear magnetic resonance spectroscopy in vivo. Int J Radiat Oncol Biol Phys 1995; 33: 719-724.
30. Vuori K, Kankaanranta L, Hakkinen AM, Gaily E, Valanne L, Granstrom ML, Joensuu H, Blomstedt G, Paetau A, Lundbom N. Low-grade gliomas and focal cortical developmental malformations: differentiation with proton MR spectroscopy. Radiology 2004; 230: 703-708.
31. Wen PY, Fine HA, Black PM, Shrieve DC, Alexander E, III, Loeffler JS. High-grade astrocytomas. Neurol Clin 1995; 13: 875-900.
32. Yeung DK, Chan Y, Leung S, Poon PM, Pang C. Detection of an intense resonance at 2.4 ppm in 1H MR spectra of patients with severe late-delayed, radiation-induced brain injuries. Magn Reson Med 2001; 45: 994-1000.